Available online at www.sciencedirect.com
SCIENCE DIRECT®
Solar Energy 74 (2003) 205–215
SOLAR ENERGY

Optimal analysis of a space solar dynamic power system

Yu-Ting Wu[a,*], Jian-Xun Ren[b], Zeng-Yuan Guo[b], Xin-Gang Liang[b]

[a]College of Environmental and Energy Engineering, Beijing University of Technology, Beijing 100022, PR China
[b]Department of Engineering Mechanics, Tsinghua University, Beijing 100084, PR China

Received 4 August 2002; received in revised form 4 March 2003; accepted 14 April 2003

Abstract

The major purpose of the present study is the theoretical modeling, numerical simulation and optimal analysis of a space solar dynamic power system. Using the method of system analysis, a mathematical and physical model is developed to describe the process of energy transfer and conversion in a space solar dynamic power system. As a new assessing criterion for total launch mass, it is proposed to combine the system mass and aerodynamic drag area into a unified criterion. The effects of the configurations and operating parameters on the system performance are analyzed and the optimal scheme of a space solar dynamic power system is obtained by numerical simulation.

Keywords: Space station; Solar energy; Dynamic power system; Configuration; Operating parameter; Numerical simulation

1. Introduction

For a variety of space missions, there exists a need for systems capable of generating power for many thousands of hours of continuous operation. Among various space solar power technologies a leading role is played by the photovoltaic (PV) cell. The second rank is designated to the so-called solar dynamic (SD) systems. Solar dynamic power was shown to offer life cycle cost advantages over photovoltaic power. The operating cost savings came primarily from:

1. elimination of batteries for eclipse power, which have relatively short lives in low earth orbit,
2. reduction in station drag area with savings in station reboost propellant due to SD's higher conversion efficiency (30–40%), and
3. less degradation in power output to end of system life.

There are three options utilized for a dynamic power system: Brayton cycle, Rankine cycle and Stirling cycle. Because the Brayton cycle is a mature technology and its efficiency is also higher than the Rankine cycle, the Brayton cycle is considered as the most promising power generation system for near future application of the space station (Glassman and Staward, 1963; Harper et al., 1990). The Brayton cycle has been applied extensively to terrestrial power systems. Most of these systems are open cycle systems used for propulsion, mechanical driving, or power generation. For application in space, the Brayton cycle must be a closed loop.

The performance of a closed Brayton cycle was evaluated using cycle efficiency and net specific power by some researchers (Wong et al., 1970; Klann, 1970; Mock, 1977). The cycle efficiency is a reflection of fuel consumption and the net specific power is usually applied to estimate the engine specific mass. For a space solar dynamic power system, solar energy is free, therefore the cycle efficiency will not directly reflect the operation economy. Net specific power reflects only the specific mass of the energy conversion component and cannot be used for assessing the dimensions or mass of the entire power system. All these facts demonstrate that cycle efficiency and net specific power are not the typical performance goals of a space solar dynamic power system.

In this paper we proposed a new assessing criterion for total launch mass, studied the effect of configurations and operating parameters on system performance, then searched for the optimal scheme of a space solar dynamic power system.

*Corresponding author. Tel.: +86-10-6739-1985.
E-mail address: wuyuting@bjpu.edu.cn (Y.-T. Wu).

0038-092X/03/$ – see front matter
doi:10.1016/S0038-092X(03)00152-X

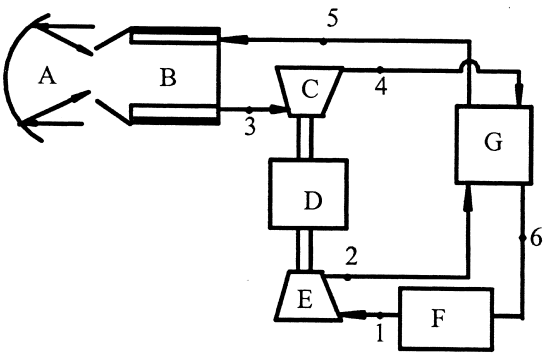

Fig. 1. Schematic diagram of system configuration. A, Concentrator; B, receiver; C, turbine; D, alternator; E, compressor; F, radiator; G, recuperator.

2. System description

Fig. 1 is a schematic diagram of a closed Brayton cycle configuration. During the insolation period, solar energy is reflected by a rotating parabolic collector toward the surface of the gas sleeve tube of the receiver. A part of the solar energy is used to heat the working gas to the design outlet temperature and the excess solar energy is stored as heat of fusion in the phase-change material. The exit gas of the receiver expands through the turbine, thereby producing the mechanical work necessary to drive the compressor and alternator, then the gas enters the recuperator where it is cooled as it transfers heat to the gas from the compressor. Final cooling of the gas takes place in the radiator, where the excess heat is rejected to space. The gas leaving the radiator is then compressed, heated in the recuperator and further heated in the heat receiver. During the following eclipse period, the stored energy in the phase-change material is withdrawn to heat the working gas for finishing the closed Brayton cycle.

The major components of the system are the solar concentrator, receiver with integrated thermal energy storage, energy conversion component, recuperator, radiator and control subsystem. For each different design, the dimensions and masses of these components are different also. The baseline configuration of this paper's example is described as follows.

1. Solar concentrator—symmetric rotation-parabolic dish.
2. Receiver—cylinder cavity receiver with the 80.5LiF–19.5CaF_2 phase-change material as the thermal energy storage salt; the configuration of the receiver is shown in Fig. 2.
3. Energy conversion component—a single-stage centrifugal compressor, a single-stage radial turbine, and smooth-rotor alternator on the same shaft.
4. Recuperator—counterflow, plate-fin heat exchanger.

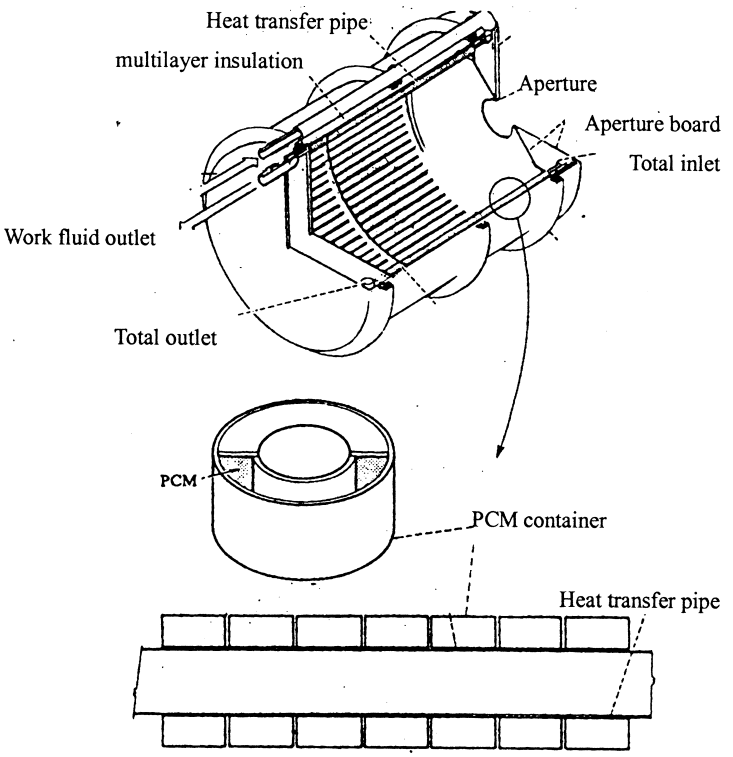

Fig. 2. The configuration of the receiver (Gietl et al., 2000).

5. Radiator—heat pipe radiator with methanol as a heat transfer liquid.

The cycle working fluid is a mixture of helium (He) and xenon (Xe).

3. System model

3.1. Choosing free variables

The first step in any optimization process is to select a set of free variables that can represent the design and operation of the system equipment. By variables analysis, the free variables in the space solar dynamic power system can be obtained. These free variables are

1. P_1, compressor inlet pressure;
2. T_1, compressor inlet temperature;
3. τ_c, compressor pressure ratio;
4. ε, recuperator effectiveness;
5. n, rotating speed;
6. N_{RC}, heat transfer pipe number of the receiver;
7. d_{RC}, heat transfer pipe diameter of the receiver;
8. d_{HRP}, heat pipe diameter of the radiator;
9. l_{HRP}, heat pipe length of the radiator;
10. hig_e, flow passage height of the cycle working fluid of the radiator.

3.2. The assessing criterion of system performance

The mass of the power system is an important performance goal that can reflect the primary energy cost and the partial launch cost. The aerodynamic drag can cause the orbit to gradually decay during the operation of the space station. To maintain the orbit altitude, thrusters have to be provided on the spacecraft. The propellant consumption of thrusters is a function of drag area. So the drag area of the power system is also an important performance goal that can reflect the maintenance energy cost and the partial launch cost. In a word, the system mass and the drag area must both be considered in order to assess effectively the power system performance.

A new assessing criterion for total launch mass is proposed to assess the system performance. Total launch mass M_L is calculated from the following equation:

$$M_L = (M_S + M_P) \tag{1}$$

where M_S is the system mass and M_P is the propellant mass for keeping the height of the space station orbit.

Total launch mass can combine system mass and the aerodynamic drag area into a unified criterion, so it is a typical performance goal of a space solar dynamic system.

3.3. System mass

The system mass may be calculated from the equation:

$$M_S = M_{SC} + M_{RC} + M_{RP} + M_{EC} + M_{HR} + M_{IV} \tag{2}$$

where M_{SC}, M_{RC}, M_{RP}, M_{EC}, M_{HR}, M_{IV} are the mass of the concentrator, receiver, recuperator, energy conversion component, radiator and auxiliary equipment, respectively.

The mass of the concentrator is

$$M_{SC} = \xi_{SC} F_{SC} \tag{3}$$

where ξ_{SC} is the specific mass of the concentrator; F_{SC} is the area of the concentrator which can be written as

$$F_{SC} = \frac{q_{SUN}}{\Omega S} \tag{4}$$

where q_{SUN} is the solar energy concentrated by the concentrator; Ω is a coefficient of the available area; S is the solar constant.

The receiver mass consists of the mass of the receiver apparatus and the mass of the phase-change salt, therefore the receiver mass can be expressed as

$$M_{RC} = \xi_{RC} F_{RC} + Q_{PCMSTOR} \cdot \tau_{sn} / r_{PCM} \tag{5}$$

where ξ_{RC} is the specific mass of the receiver; $Q_{PCMSTOR}$ is the energy rate stored in the phase-change material in the sun period; r_{PCM} is the melting latent heat of the phase-change material; τ_{sn} is the sun period length; F_{RC} is the area of the receiver heat transfer pipes which can be calculated by

$$F_{RC} = N_{RC} \pi d_{RC} l_{RC} = \frac{W C_p \ln\left(\dfrac{T_W - T_3}{T_W - T_5}\right)}{h} \tag{6}$$

where N_{RC}, d_{RC}, l_C are the number, diameter and length of the receiver, respectively; W, C_p are mass flow rate and specific heat of the work fluid, respectively; h is the convection heat transfer efficiency; T_W, T_3, T_5 are the temperature of the wall, inlet and outlet of the heat transfer pipe of the receiver, respectively.

The recuperator mass can be obtained by:

$$M_{RP} = \xi_{RP} F_{RP} \tag{7}$$

where ξ_{RP} is the specific mass of the recuperator; F_{RP} is the recuperator area that can be calculated by

$$F_{RP} = \frac{W C_p}{U \cdot \mathrm{NTU}} \tag{8}$$

where U is the overall coefficient of heat transfer; NTU is the number of transfer unit.

The mass of the energy conversion component can be written as

$$M_{EC} = \xi_{EC} D_C^2 \tag{9}$$

where ξ_{EC} is the specific mass of the energy conversion unit; D_C is the diameter of the compressor which can be calculated by

$$D_C = \frac{\sqrt{c_p (T_2 - T_1)/\psi}}{\pi n} \tag{10}$$

where T_2, T_1 are outlet and inlet temperature of the compressor, respectively; ψ is the compressor head coefficient; n is the rotating speed of the compressor.

The radiator is composed of a heat pipe, fin and exchanger, so its mass equation is

$$M_{HR} = \xi_{HRF}F_{HRF} + \xi_{HRH}F_{HRH} + \xi_{HRP}F_{HRP} \quad (11)$$

$$F_{HRF} = N_{HR}l_c W_{HRF} \quad (12)$$

$$F_{HRP} = \pi d_{HR}(4l_e + l_c) \quad (13)$$

$$F_{HRH} = 2N_{HR}W_{HRF}(\mathrm{wid}_{HRH} + \mathrm{hig}_{HRH}) \quad (14)$$

where ξ_{HRF}, ξ_{HRH}, ξ_{HRP} are the specific mass of the fin, heat exchanger and heat pipe of the radiator, respectively; F_{HRF}, F_{HRH}, F_{HRP} are the area of the fin, heat exchanger and heat pipe of the radiator, respectively; N_{HR}, l_e, l_c are the number, vaporizer length and condenser length of the heat pipe, respectively; W_{HRF} is the width of the radiator fin; wid_{HRH}, hig_{HRH} are the width and height of the heat exchanger, respectively.

The mass of auxiliary equipment is calculated by

$$M_{IV} = \xi_{IV}Na \quad (15)$$

where ξ_{IV} is the specific mass of auxiliary equipment; Na is the output power of the system.

3.4. Propellant mass

The aerodynamic drag area F_p of a space solar dynamic power system may be obtained from

$$F_p = F_{SC} + 0.5F_{HRF}. \quad (16)$$

The propellant mass for keeping the height of the space station orbit can be calculated from

$$M_p = \frac{c_{ear}C_D F_p \rho}{2I_{SP}r}\tau \quad (17)$$

where c_{ear} is a constant of earth gravitation; C_D is the resistant factor; I_{SP} is the specific propulsion of the engine keeping orbit altitude; r is the distance from the system to the core of earth; τ is the system life; ρ is the atmosphere density on the orbit.

3.5. Search method

The direct search method is used in this study, because the assessing criterion is an implicit nonlinear function of free variables and it is difficult to obtain its differential coefficient. The study applies the coordinate descent method to search the optimal value of free variables.

The coordinate descent method is to cycle through the n coordinate directions $x_1, x_2, \ldots, x_n$, using each in turn as a search direction. At the first iteration, we fix all except the first variable, and find a new value of this variable that minimizes the objective function. On the next iteration, we repeat the process with the second variables, and so on. After n iterations, we return to the first variable and repeat the cycle.

4. Results and discussion

The computer program described in previous sections is used to perform the parametric study and the global optimization study for a 10 kW power system. The main parameters used in the calculations in this paper are given in Table 1 (Dong, 1998; Diao, 1992).

Table 1
Main parameters of the power system in this study

Parameters	Values
m_w, molecular weight of working fluid	39.94
T_3, turbine inlet temperature, K	1040
T_s, heat sink temperature, K	223
T_{RCW}, the wall temperature of heat transfer pipe of receiver, K	1053.15
τ_{sn}, insolation period, min	58
τ_{sh}, eclipse period, min	36
r_{pcm}, fusion latent heat of phase change salt, J/kg	790 000
S, solar constant, kW/m^2	1353
ξ_{SC}, concentrator specific mass, kg/m^2	2.65
ξ_{RC} receiver specific mass, kg/m^2	130
ξ_{RP}, recuperator specific mass, kg/m^2	1.80
ξ_{EC}, energy conversion component specific mass, kg/m^2	5360
ξ_{HRF}, radiator fin specific mass, kg/m^2	2.21
ξ_{HRP}, radiator heat pipe specific mass, kg/m^2	9.23
ξ_{HRH}, radiator exchanger specific mass, kg/m^2	5.9
τ, the system life, s	6.3072×10^8

4.1. Effect of operating parameters on system performance

The main operation parameters of the solar closed Brayton cycle system include compressor inlet temperature, compressor inlet pressure, compressor pressure ratio, rotating speed of energy conversion component and recuperator effectiveness. Taking a 10 kW solar dynamic space power system as an example, we will give a detailed discussion on the effects of these parameters on system performance.

4.1.1. Effect of compressor inlet temperature

Fig. 3 shows the effect of compressor inlet temperature on the mass of each component. As the compressor inlet temperature increases, the masses of the concentrator, receiver and energy conversion component increase gradually, whereas the mass of the radiator decreases gradually. For a given set of other parameters, the increase of the compressor inlet temperature causes a decrease in cycle specific work and heat efficiency, which increases the masses of the energy conversion component, receiver and concentrator. On the other hand, the increase of the inlet temperature can reduce the rejection heat of the radiator, thus reducing the radiator mass.

The effect of compressor inlet temperature on system performance is illustrated in Figs. 4 and 5. It is seen from Fig. 5 that there is an optimal value of inlet temperature in the system. At the inlet temperature of 280 K, the total launch mass reaches its minimum value of 2029 kg in which the system mass, the average total launch mass and drag area are 1157 kg, 2106 kg and 57 m^2, respectively. So the optimization of the compressor inlet temperature can result in a decrease of 3.8% in total launch mass

4.1.2. Effect of compressor inlet pressure

Inlet pressure affects the density of working fluid. Higher density helps to raise the system heat-transfer capability but reduce the efficiency of the compressor and turbine. It can be seen from Fig. 6 that the mass of the concentrator, receiver, radiator and recuperator decreases initially and then increases as compressor inlet pressure increases, so there is an optimal value of inlet pressure. This is because the heat-transfer capability of the working fluid increases as the compressor inlet pressure increases, thus reduces the mass of each component initially; but when the pressure increases to a certain value, the efficiency of the compressor and turbine decreases sharply,

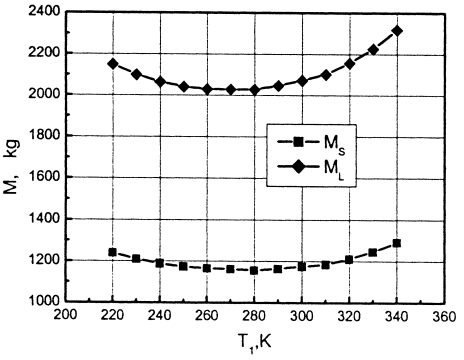

Fig. 4. Effect of compressor inlet temperature on system mass and total launch mass.

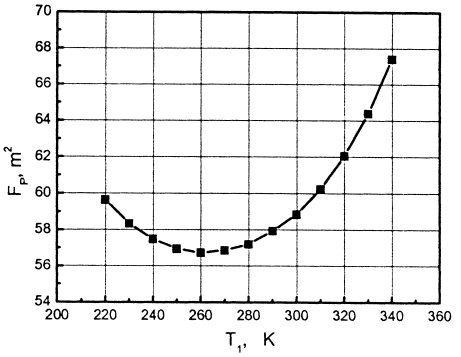

Fig. 5. Effect of compressor inlet temperature on drag area.

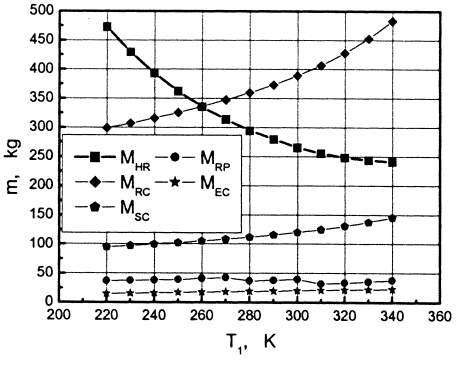

Fig. 3. Relationship of compressor inlet temperature and mass of each component.

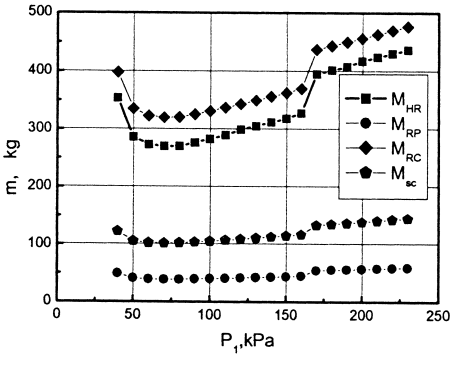

Fig. 6. Relationship of compressor inlet pressure and mass of each component.

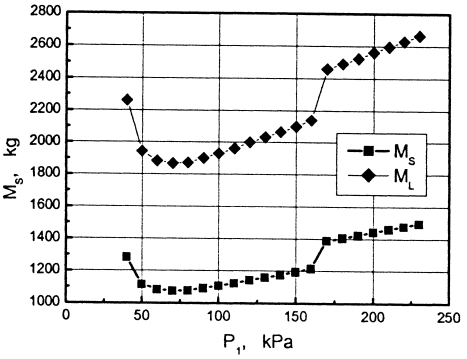

Fig. 7. Effect of compressor inlet pressure on system mass and total launch mass.

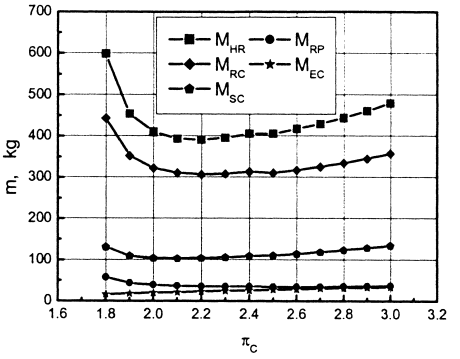

Fig. 9. Relationship of compressor pressure ratio and mass of each component.

which reduces the cycle heat efficiency and finally raises the mass of each component.

The effect of compressor inlet pressure on system performance is shown in Figs. 7 and 8. An optimal value exists for the inlet pressure. At the compressor inlet pressure of 70 kPa, the total launch mass reaches its minimum value of 1870 kg, for which the average launch mass, system mass and drag area are 2196 kg, 1870 kg and 52.1 m^2, respectively. So the optimization of the compressor inlet pressure can lead to a decrease of 17.4% in total launch mass.

4.1.3. Effect of compressor pressure ratio

For a given set of other parameters, the change of the pressure ratio of the compressor will affect the flow rates of the system cycle working fluid, and therefore affect the performance of the system and its components, as shown in Figs. 9–11. From Fig. 9 we can find that as the pressure ratio of the compressor increases, on the one hand, the mass of the energy conversion component increases gradually, on the other hand, the mass of the concentrator, heat receiver, recuperator and radiator decrease initially and

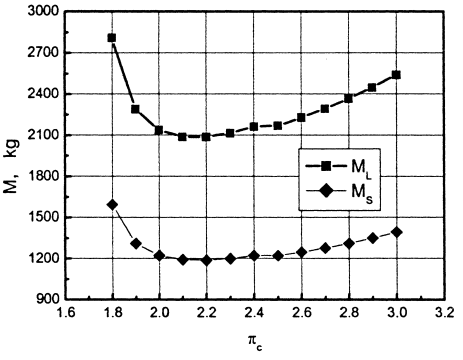

Fig. 10. Effect of compressor pressure ratio on system mass and total launch mass.

then increase gradually after reaching its respective minimum value at $\pi_c = 2.1$.

Fig. 11 indicates that the optimal value of compressor pressure ratio is 2.1, for which the system mass, drag area, total launch mass and average launch mass are 1193 kg, 59 m^2, 2089 kg and 2289 kg, respectively. So by optimizing the compressor pressure ratio, the total launch mass can be decreased by 9.6%.

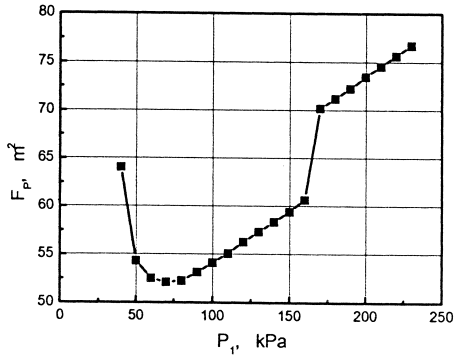

Fig. 8. Effect of compressor inlet pressure on drag area.

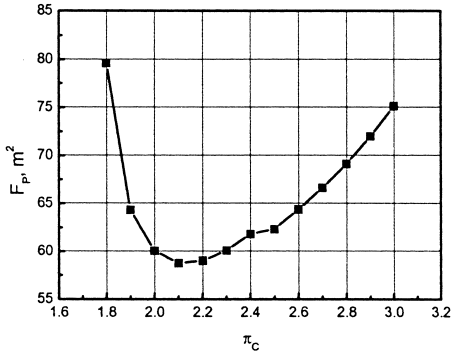

Fig. 11. Effect of compressor pressure ratio on resistance area.

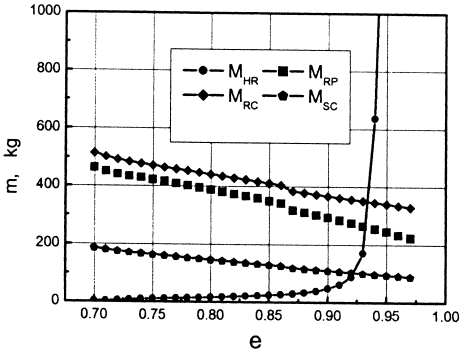

Fig. 12. Relationship of recuperator effectiveness and mass of each component.

4.1.4. Effect of recuperator effectiveness

Fig. 12 illustrates the effect of recuperator effectiveness on mass of each component. It is evident from the figure that high recuperator effectiveness reduces the temperature difference of the recuperator and worsens the heat transfer, which makes the recuperator mass increase as recuperator effectiveness increases. Especially for recuperator effectiveness above 0.93, the recuperator mass of the heat regenerator increases sharply as recuperator effectiveness increases. On the other hand, increase of recuperator can raise the cycle thermal efficiency, thus lower the mass of the concentrator, receiver and radiator.

Figs. 13 and 14 show the effect of recuperator effectiveness on system performance. It can be seen from Fig. 13 that the total launch mass decreases initially and then increases sharply as the recuperator effectiveness rises. When the recuperator effectiveness is 0.92, the total launch mass reaches its minimum value of 1972 kg, at which its average value, the system mass and drag area are 2835 kg, 1167 kg and 53 m^2, respectively. So the optimization on recuperator effectiveness can reduce the total launch mass by 43.7%.

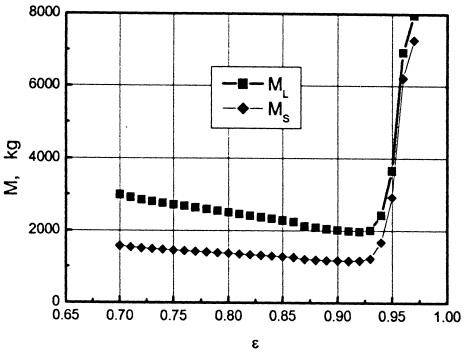

Fig. 13. Effect of recuperator effectiveness on system mass and total launch mass.

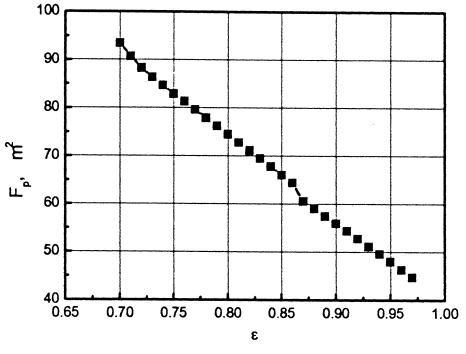

Fig. 14. Effect of recuperator effectiveness on drag area.

4.2. Effect of configuration on system performance

For a solar dynamic power system, its main configuration includes diameter and number of the heat-transfer pipe of the heat receiver, diameter and length of the heat pipe of the radiator and flow passage height of the cycle working fluid in the radiator. Taking a 10 kW solar dynamic space power system for example, we will discuss in detail the effect of these parameters on performance of the system and components.

4.2.1. Effect of heat-transfer pipe diameter of receiver

Reduction of the heat-transfer pipe diameter of the receiver can improve the heat-transfer efficiency of the working fluid, but at the same time it will raise the flowing drag of the cycle working fluid, and thus affect the cycle efficiency of the whole system. Fig. 15 shows that the mass of the receiver increases as the heat-transfer pipe diameter increases, but the masses of the radiator and concentrator decrease as the diameter increases.

The effect of the heat-transfer pipe diameter on system performance is shown in Figs. 16 and 17. From the figures we can find that as the pipe diameter increases, the system mass is reduced to the lowest point and then increases, but the drag area decreases all the time. Fig. 17 indicates that when the heat transfer pipe diameter is 14 mm, the total launch mass reaches its minimum value of 1843 kg in which the average total launch mass, system mass and drag area are 1929 kg, 987 kg and 56 m^2. So the optimization on the heat-transfer pipe diameter can reduce the total launch mass by 4.7%.

4.2.2. Effect of heat-transfer pipe number of receiver

Receiver mass is directly determined by the number of the heat-transfer pipe. The smaller the number is, the smaller the receiver mass is. But the decrease of the number of heat-transfer pipe will raise the flow rate through each heat-transfer pipe, thus raise the flowing drag of the working fluid and lower the heat efficiency of the whole system, then finally increase the mass of other components. Figs. 18–20 show the effect of the number of

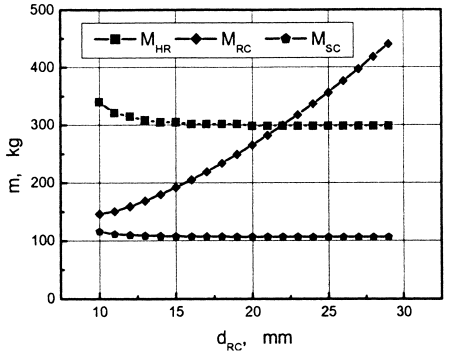

Fig. 15. Relationship of heat-transfer pipe diameter and mass of each component.

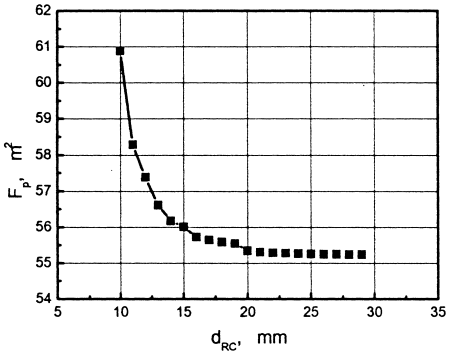

Fig. 16. Effect of heat-transfer pipe diameter on drag area.

heat-transfer pipe on the mass of system and components. These figures indicate that as the number of heat-transfer pipe increases the receiver mass increases linearly, but the recuperator masses, radiator mass, concentrator mass and the drag area decrease initially, but after attaining the minimum at a certain number of pipes, they remain constant. System mass and total launch mass decrease initially and then increase as the number of pipes increases. Fig. 19 shows that when the number of pipes is set at 16,

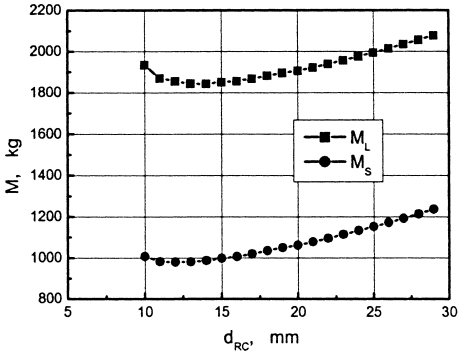

Fig. 17. Effect of heat-transfer pipe diameter on system mass and total launch mass.

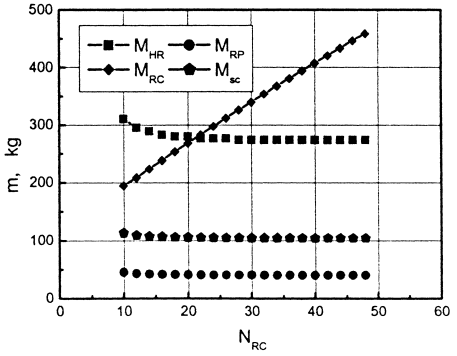

Fig. 18. Relationship of heat-transfer pipe number and mass of each component.

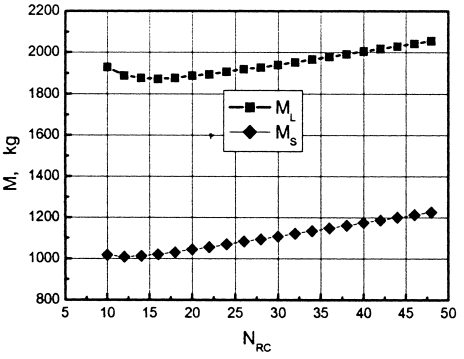

Fig. 19. Effect of heat-transfer pipe number on system mass and total launch mass.

total launch mass has its minimum value of 1873 kg, in which the average total launch mass, system mass and drag area are 1948 kg, 1021 kg and 55.9 m^2. By optimizing the number of heat-transfer pipes, total launch mass will decrease by 4.0%.

4.2.3. Effect of heat pipe length of radiator

Figs. 21–23 show the effect of heat pipe length of the radiator on the masses of system and components. The

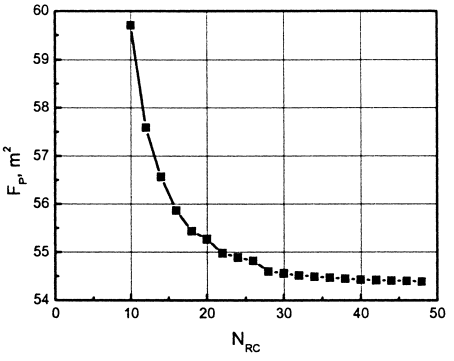

Fig. 20. Effect of heat-transfer pipe number on resistance area.

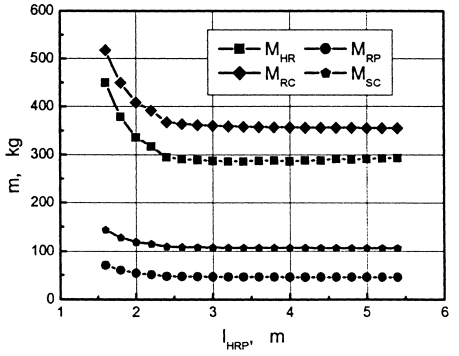

Fig. 21. Relationship of heat pipe length and mass of each component.

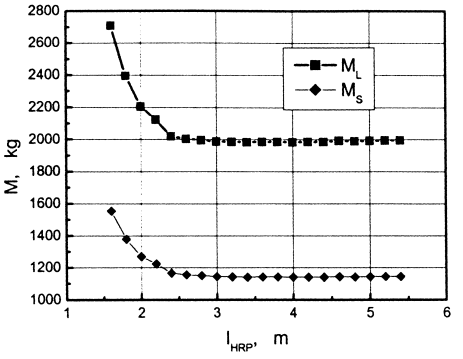

Fig. 22. Effect of heat-pipe length on system mass and total launch mass.

mass of the radiator decreases initially and then increases as the length of the heat pipe increases. But as the length increases the masses of heat recuperator, concentrator and heat receiver decrease initially, but after attaining the minimum at a certain value, they remain constant without an effect of the pipe length. System mass, drag area and total launch mass decrease initially and then rise as the length of the heat pipe rises. When the length of the heat pipe is set at 3.4 m, total launch mass has its minimum

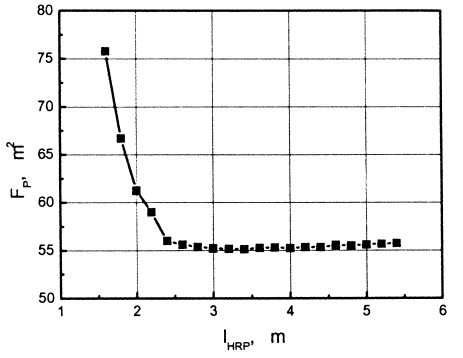

Fig. 23. Effect of heat-pipe length on drag area.

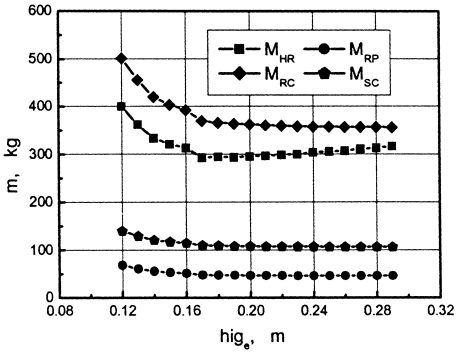

Fig. 24. Relationship of flow passage height and mass of each component.

value of 1983 kg, in which the average total launch mass, system mass and drag area are 2065 kg, 1142 kg and 55.1 m^2. So the optimization on the length of the heat pipe will reduce the total launch mass by 4.1%.

4.2.4. Effect of the flow passage height of the cycle working fluid

Increase in the height of the cycle working fluid will reduce the flowing drag of the cycle working fluid, promote cycle heat efficiency, but reduce the convection heat-transfer efficiency of the heat pipe. So as the flow passage height of the cycle working fluid rises, the mass of the concentrator, receiver and recuperator decreases gradually, but the mass of the radiator decreases initially and then increases (refer to Fig. 24).

Figs. 25 and 26 show the effect of the height of the cycle working fluid on the system performance. As seen in the figures, system mass, drag area and total launch mass all decrease initially and then increase as flow passage height increases. When the height is set at 0.23 m, the total launch mass reaches its minimum value of 1999 kg, in which the average value of the total launch mass, the system mass and drag area are 2091 kg, 1159 kg and 55.1 m^2. So by optimizing the flow passage height of the

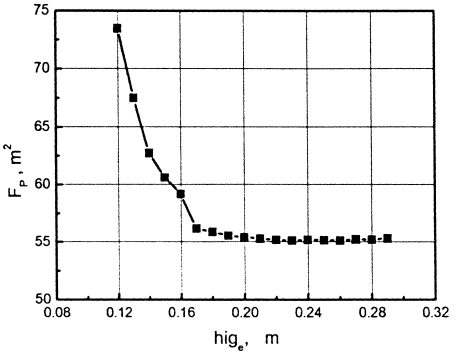

Fig. 25. Effect of flow passage height on drag area.

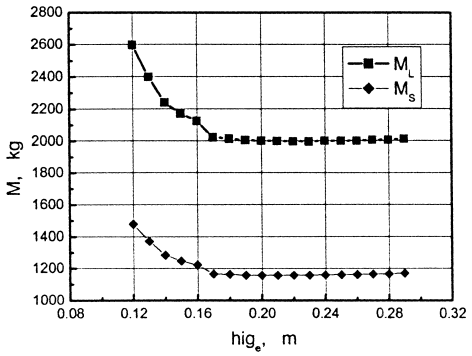

Fig. 26. Effect of flow passage height on system mass and total launch mass.

cycle working fluid, the total launch mass will decrease by 4.6%.

4.3. Effect of waste heat utilization on system performance

The exhaust heat of a solar dynamic space power system needs to be rejected to the space by the radiator, however the electrical heating appliances are needed by the other systems of the space station, such as the CO_2 removal system, ventilation system, urine disposal system, etc. If the exhaust heat can be effectively utilized, then some of the electrical heating appliances will be unnecessary, consequently, the power consumption, system mass and drag area of the power system may be reduced. Taking a 10 kW solar dynamic space power system for example, we have compared two programs, one utilizes exhaust heat, and the other does not. The calculated total launch mass, system mass and drag area are 2148 kg, 1138 kg and 66.3 m^2, respectively, for the latter case. While 2 kW heat is led out from the exit of the heat recuperator to the other systems of the space station, the total launch mass, system mass and drag area will be reduced to 1751 kg, 960.5 kg, and 51.9 m^2, respectively. The total launch mass is reduced by 22.7%. It is clear that making use of exhaust heat can reduce the system mass and drag area.

4.4. Global optimization result

The global optimization was made for a solar dynamic power system with power output of 10 kW. Table 2 shows the search range and optimum of the free variables and Table 3 is the mass of units and system in the optimum and worst operating mode. From Table 2, it can be seen that the minimum total launch mass is 1640.47 kg and the maximum is 6156.89 kg in the range of the free variables shown in Table 2. The average total launch mass is 1822.86 kg. By global optimization, the total launch mass can decrease by 11.1%. In addition, Table 3 indicates that propellant mass is 50% of total launch mass, so it takes a large proportion of the total cost of the power system. The evaluation criterion of total launch mass not only represents the effect of system mass but also considers the space operational behavior of the space power system, so total launch mass is a valuable tool for space power system design.

Table 2
Search range and optimum of parameters

Parameter	P_1 (kPa)	T_1 (K)	n (r/s)	π_C	ε
Search range	60–160	240–320	800–1400	1.6–2.3	0.80–0.97
Optimum	70	270	1400	1.8	0.92
Parameter	d_{HRP} (mm)	hig_{HRH} (m)	l_{HRP} (m)	N_{RC}	d_{RC} (mm)
Search range	12–32	0.1–0.3	2.0–4	16–36	12–32
Optimum	12	0.23	3.8	26	18

Table 3
The mass of units and system in the optimum and worst operating mode

Operating mode	M_{SC} (kg)	M_{RC} (kg)	M_{EC} (kg)	M_{RC} (kg)	
Optimum	95.68	176.21	15.88	71.63	
Worst	354.22	828.38	15.97	327.65	
Operating mode	M_{HR} (kg)	M_S (kg)	M_P (kg)	F_P (m^2)	M_L (kg)
Optimum	225.91	835.32	793.10	52.04	1628.41
Worst	1133.44	2909.65	3247.24	213.07	6156.89

5. Conclusions

This study demonstrated that the thermal management study of a solar dynamic space power system can obtain notable benefit with respect to weight reduction and also is instructive in the design of solar dynamic space power systems. The results of this investigation may be summarized as follows.

1. A mathematical model for evaluating the system mass was developed and a computer program for use in optimizing a solar dynamic space power system was created based on the model.
2. A new assessing criterion relating to the total launch mass is introduced, which combines the system mass and the aerodynamic drag area into a unified criterion. The results support that the new criterion, total launch mass, is a valuable tool for space power system design.
3. There are both positive and negative effects of operating and configuration parameters on the whole system and the optimization of these parameters can reduce the total launch mass.
4. Based on the analysis of energy consumption of other systems in the space station, a scheme of waste heat utilization is proposed to replace the electrical heating appliances in other systems. The results indicate that waste heat utilization cannot save power consumption, but also reduce total launch mass by 22.7% in the 10 kW solar dynamic system.
5. By global optimization, the optimum value of free variables are obtained and total launch mass can decrease by 11.1%.

References

Diao, Z.-G., 1992. Performance evaluation of space solar Brayton cycle power system. ASME, 92-GT-96.

Dong, K.Y., 1998. Thermal Analysis of High Temperature Solid–Liquid Phase Change Thermal Energy Storage Container[D]. Beijing University of Aeronautics and Astronautics, Beijing.

Gietl, E.B., Gholdston, E.W., Cohen, F. et al., 2000. The architecture of the electric power system of the international space station and its application as a platform for power technology development. AIAA, 2954.

Glassman, A.J., Staward, W.I., 1963. A look at the thermodynamic characteristics of brayton cycle for space power. AIAA 63, 218.

Harper, W.B., Boyle, V.B., Kudija, C.T., 1990. Solar dynamic CBC power for space station freedom[R]. ASME, Paper 90-GT-78.

Klann, L.J., 1970. Steady-state analysis of a Brayton space power system. NASA, TN D-5673.

Mock, E.A., 1977. Closed cycle gas turbine optimization-procedures and examples. Airesearch Report 31, 2635.

Wong, R.Y., Klassen, H.A., Evans, R.C., 1970. Effect of operating parameters on net power output of a 2-to-10-kilowatt Brayton rotating component. NASA, TN D-5815.